Self-consistent phonons, thermal properties, and vibrational instability of the copper crystal

C. S. Jayanthi,* E. Tosatti, and A. Fasolino
International School for Advanced Studies (ISAS), 34014 Trieste, Italy
(Received 5 April 1984)

We have studied the temperature-dependent phonon spectrum and other vibrational properties of copper using the self-consistent phonon method and also the quasiharmonic method. A model pair potential suitable for such a study has been constructed. We have also investigated the vibrational instability of the overheated perfect crystal by studying the system's free energy.

I. INTRODUCTION

The work reported in this paper has three distinct scopes. First, we study the thermal properties of copper crystal using the self-consistent phonon method[1] (SCP) and also the quasiharmonic[1] (QH) method. Both these approaches are based on a pairwise, central, short-ranged potential. This choice excludes several potential forms that have been previously constructed to account for various properties of Cu, either starting from first principles,[2–5] or empirical.[6,7] These forms are either explicitly or implicitly long ranged and do not easily lend themselves to a simple calculation of thermal properties. The second scope of this work is to show that by careful choice of the pair potential the above two methods can be made to give similar thermal properties. A general choice of pair potential would, of course, not satisfy this requirement, as exemplified in Ref. 7. As discussed in a later section, the disagreement between QH and SCP is not generally a necessity and it is easily possible to eliminate it. Once this result is established, one can use the simpler and cruder QH method for more complicated studies, such as the study of the thermal properties of copper surfaces,[8] where it would not be an easy task to implement the SCP method. The third scope of this paper is to use the free energies of the SCP and QH theories to study the vibrational instability, which the crystal would undergo at high temperatures, should it somehow be prevented from melting. This instability is associated with the loss of the local crystalline free-energy minimum and will occur quite generally for any solid, corresponding to the maximum temperature at which the ideally defect-free crystal can be overheated. Such an instability is also well known to occur in self-consistent phonon theories[9] well above melting.[10] Although distinct in principle, and different numerically from the true melting temperature, the self-consistent instability temperature is nevertheless a good indicator of the relative tendency to melt in a given class of similar crystals.[11] While we do not plan such a study here, it seems interesting to establish an explicit connection between a short-range potential modeling a *metal* crystal and the lattice instability it generates. In particular, we find that, in copper, instability and melting can be much closer than in a rare-gas solid.[10] Another motivation for studying this kind of bulk instability is that it provides a starting point for subsequent studies of surface melting based on lattice instabilities.[12,8]

The central ingredient to this work is the pair potential that is chosen empirically to correctly reproduce the temperature-dependent lattice-dynamical properties of copper. At this point we shall pause briefly to discuss the basic difficulty in choosing a two-body short-ranged potential for metals. The pair potentials that were proposed previously[13–15] were constructed with purposes of yielding reasonable cohesive and defect properties and of describing the lattice dynamics at $T=0$. It is well known, however, that cohesion in metals arises because of the competition between many-body attractive electronic forces and essentially two-body core-core repulsion. Therefore any attempt to describe cohesion in metals using a two-body potential is intrinsically incorrect. If one insists on such a description, one is forced to choose an unusually deep potential. The result is, that such a potential will as a rule yield incorrect thermal properties.

For the purpose of the present investigation we finally choose a shallow two-body potential which is good for describing thermal properties and bad for describing cohesion. This problem does not exist in rare-gas solids, where cohesion is satisfactorily described by a pair potential. In our case only a small fraction of the total cohesion is accounted for by the pair potential. This can be rationalized by considering, for example, the ratio

$$C=(\text{cohesive energy per atom})/k_B T_M \ ,$$

where T_M is the melting temperature. In the rare-gas crystals, $C\simeq 10$. In Cu, however, $C\simeq 30$, and it can be even higher in other fcc metals (e.g., 40 in Al). If we assume, as a first guess, that at melting only the pairwise energy increases (the total electron density being essentially unchanged), then $(C-10)/C$ can be seen as crudely representing the fraction of cohesion not due to pairwise forces. The fact that $(C-10)/C$ is large, of the order $\frac{2}{3}$ in Cu, then justifies *a posteriori* our finding that the thermal properties of metals are the best represented by a shallow pairwise potential.

The plan of the paper is as follows. We present in Sec. II the standard SCP and QH formulas, as well as some of the relevant details of our calculation. In Sec. III we deal with optimizing the pair potential to represent copper. Finally, in Sec. IV we report the numerical results of our calculation together with a discussion of them and our conclusions.

II. SELF-CONSISTENT PHONON CALCULATION AND QUASIHARMONIC CALCULATION

Given a Hamiltonian

$$H=\sum_i \frac{P_i^2}{2M}+\tfrac{1}{2}\sum_{i,j} V(|\vec{R}_i-\vec{R}_j|)\,, \tag{2.1}$$

the true free energy $F=-\beta \ln \mathrm{Tr}\, e^{-\beta H}$ $(\beta=1/k_B T)$ is variationally approximated by

$$F_0=-\beta \ln \mathrm{Tr}\, e^{-\beta H_0}\,, \tag{2.2}$$

where H_0 is an approximate trial harmonic Hamiltonian, given by

$$H_0=\sum_i \frac{P_i^2}{2M}+\tfrac{1}{4}\sum_{i,j} \vec{u}_i\cdot\overleftrightarrow{D}_{ij}\cdot\vec{u}_j\,, \tag{2.3}$$

$\vec{u}_i$ being the displacement of the ith atom from its equilibrium position, and D is a dynamical matrix whose parameters are adjustable. Variational optimization of F_0 yields, for the best "self-consistent" dynamical matrix, the well-known formula[1]

$$\overleftrightarrow{D}_{ij}(T)=\langle \vec{\nabla}_i \vec{\nabla}_j V_{ij}\rangle_T\,, \tag{2.4}$$

where the thermal average is meant to be self-consistently taken over the harmonic states of H_0, i.e., of D_{ij} itself. For a general quantity $g(\vec{R}_i-\vec{R}_j)$, such an average can be written as

$$\begin{aligned}\langle g(\vec{R}_i-\vec{R}_j)\rangle &= \sum_{\vec{q}} g(\vec{q})\langle e^{i\vec{q}\cdot(\vec{R}_i-\vec{R}_j)}\rangle \\ &\simeq \sum_{\vec{q}} g(\vec{q})\exp[i\vec{q}\cdot(\vec{R}_i^{\,0}-\vec{R}_j^{\,0})] \\ &\quad\times\exp[-\tfrac{1}{2}\langle|\vec{q}\cdot(\vec{u}_i-\vec{u}_j)|^2\rangle]\,,\end{aligned} \tag{2.5}$$

where $g(\vec{q})$ is the Fourier transform of $g(\vec{R})$, and $\vec{R}=\vec{R}_i-\vec{R}_j$, with $\vec{R}_i=\vec{R}_i^{\,0}+\vec{u}_i$, and $\vec{R}_i^{\,0}$ is the equilibrium position of the ith atom. In what follows we shall also use the concise notation $\vec{R}^{\,0}$, $\vec{u}$ for convenience in representing the relative equilibrium distance $(\vec{R}_i^{\,0}-\vec{R}_j^{\,0})$ and the relative displacement $(\vec{u}_i-\vec{u}_j)$ between first-neighbor atoms i and j.

Considering a central, first-neighbor pair potential, we can explicitly write the expression for the dynamical matrix in Eq. (2.4) as

$$D_{\mu\nu}=\langle\alpha\delta_{\mu\nu}\rangle+\left\langle(\beta-\alpha)\frac{R_\mu R_\nu}{|R|^2}\right\rangle\,. \tag{2.6}$$

Here, $\alpha(R)=R^{-1}[\partial V(R)/\partial R]$ and $\beta(R)=\partial^2 V(R)/\partial R^2$ are the first- and second-order force constants. Performing the second average in Eq. (2.6) with general prescription (2.5), which involves using the Fourier transform of $(\beta-\alpha)R_\mu R_\nu/|R|^2$, is not straightforward. We approximately factorize that average in the form

$$\langle(\beta-\alpha)R_\mu R_\nu/|R|^2\rangle\simeq\langle\beta-\alpha\rangle\langle R_\mu R_\nu/|R|^2\rangle\,. \tag{2.7}$$

The first factor, $\langle\beta-\alpha\rangle$, can then be evaluated with Eq. (2.5). The second average can be expressed directly, to second order in u, as

$$\begin{aligned}\left\langle\frac{R_\mu R_\nu}{|R|^2}\right\rangle &\simeq \frac{R_\mu^0 R_\nu^0}{|R^0|^2}-\langle|u|^2\rangle\frac{R_\mu^0 R_\nu^0}{|R^0|^4} \\ &\quad+\frac{\langle u_\mu u_\nu\rangle}{|R^0|^2}-2\frac{\langle\vec{R}^{\,0}\cdot\vec{u})u_\mu\rangle}{|R^0|^4}R_\nu^0\,.\end{aligned} \tag{2.8}$$

To this order, the factorization (2.7) is actually exact, as is shown in Appendix A. The explicit form of the dynamical matrix for fcc crystals calculated with the above set of approximations is given in Appendix B.

It is evident from Eq. (2.5) that evaluation of averages like $\langle\alpha\rangle$ and $\langle\beta\rangle$ primarily involves calculation of the quantity

$$\begin{aligned}\langle|\hat{q}\cdot\vec{u}|^2\rangle &= \frac{\hbar}{NM}\sum_{\vec{k},\lambda}\frac{|\hat{q}\cdot\hat{e}(\vec{k},\lambda)|^2}{\omega_{\vec{k}\lambda}} \\ &\quad\times(1-\cos\vec{k}\cdot\vec{R}^{\,0})\frac{\coth(\beta\hbar\omega_{\vec{k}\lambda})}{2\beta}\,.\end{aligned} \tag{2.9}$$

We have similar expressions for other averages like $\langle u_\mu u_\nu\rangle$. The summation in Eq. (2.9) is over all the normal modes of frequency $\omega_{\vec{k}\lambda}$ and polarization vector $\hat{e}(\vec{k},\lambda)$ that are obtained as solutions of the eigenvalue equation

$$\sum_\nu[D_{\mu\nu}(\vec{k})-M\omega^2(\vec{k},\lambda)\delta_{\mu\nu}]\hat{e}_\nu(\vec{k},\lambda)\,. \tag{2.10}$$

The Brillouin-zone summation in Eq. (2.9) is done with 256 mean-value points.[16] This average $\langle|\hat{q}\cdot\vec{u}|^2\rangle$ is calculated for $\hat{q}$ along the [100], [110], and [111] directions, and for various first-neighbor positions. The result obtained at $T=500$ K is given in Table I. We note that the mean value of this average is close to the one obtained for $\hat{q}\|[110]$ and $\vec{R}^{\,0}\|[101]$. Thus, we choose this direction in our subsequent evaluation of the quantity $\exp(-\frac{1}{2}\langle|\vec{q}\cdot\vec{u}|^2\rangle$ appearing in Eq. (2.5) and neglect all other directional dependences. With this approximation, we have

TABLE I. $\langle|\hat{q}\cdot\vec{u}|^2\rangle$ calculated for various orientations of the $\hat{q}$ vector, $\vec{u}$ being the relative displacement of first-neighbor atoms, separated by $\vec{R}^{\,0}$. All other directions are related by symmetry. The temperature used was 500 K.

$\hat{q}$	$\vec{R}^{\,0}$	$\langle\lvert\hat{q}\cdot\vec{u}\rvert^2\rangle$ (Å^{-2})
(1,0,0)	(1,1,0)	0.0150
	(0,1,1)	0.0163
$(1,1,0)/\sqrt{2}$	(1,0,1)	0.0159
	(1,1,0)	0.0129
	(−1,1,0)	0.0170
$(1,1,1)/\sqrt{3}$	(0,−1,−1)	0.0141
	(1,−1,0)	0.0168

$$\langle\alpha(\vec{R})\rangle=\sum_{\vec{q}}\alpha(\vec{q})\exp\left[-\frac{q^2}{2}\left\langle\left|\left[\frac{1}{\sqrt{2}},\frac{1}{\sqrt{2}},0\right]\cdot\vec{u}\right|^2\right\rangle\right]$$

$$\times\exp(i\vec{q}\cdot\vec{R}^0)\ , \tag{2.11}$$

with

$$\alpha(\vec{q})=\frac{1}{\Omega}\int d^3R\,\alpha(\vec{R})e^{-i\vec{q}\cdot\vec{R}}\ ,$$

and a similar expression for $\langle\beta(\vec{R})\rangle$. The values of $\alpha(q)$ and $\beta(q)$ are calculated from the empirical values assumed for $\beta(R)$, used in the construction of the pair potential and from

$$\alpha(R)=\frac{1}{R}\int_{R_0=a_0/\sqrt{2}}^{R}\beta(r')dr'\ .$$

The values of $\alpha(q)$ and $\beta(q)$ are then stored for later use in the averaging.

Our scheme for the SCP calculation involves solving Eqs. (2.7)—(2.11) self-consistently for each given temperature T and crystal lattice spacing a. More explicitly, for a given T and a, we (i) choose a trial initial value for α and β; (ii) diagonalize the 3×3 dynamical matrix in Eq. (2.10) to find $\omega_{\vec{k}\lambda}$ and $\hat{e}_{\vec{k}\lambda}$; (iii) use these eigenvalues and eigenvectors to calculate averages like $\langle|u|^2\rangle$, $\langle|\vec{q}\cdot\vec{u}|^2\rangle$, $\langle u_\lambda u_\nu\rangle$, and finally $\langle\alpha\rangle$ and $\langle\beta\rangle$; and (iv) feed back these $\langle\alpha\rangle$ and $\langle\beta\rangle$ as new input values and then repeat the entire cycle until the difference in value of these quantities between consecutive steps becomes negligible. The self-consistent free energy is then given by

$$F_{\rm SCP}=\tfrac{1}{2}\sum_{i,j}\langle V(|\vec{R}_i-\vec{R}_j|)\rangle$$
$$+\beta^{-1}\sum_{\vec{k},\lambda}\left[\ln 2\sinh\left[\frac{\beta\hbar\omega_{\vec{k}\lambda}}{2}\right]-\beta\frac{\hbar\omega_{\vec{k}\lambda}}{4}\coth\left[\frac{\beta\hbar\omega_{\vec{k}\lambda}}{2}\right]\right], \tag{2.12}$$

TABLE II. Fourier transform of the potential B. Units of q and V are $2\pi/a$ and eV, respectively.

q	$V(q)$	q	$V(q)$
0.0	$0.141\,058\,12\times10^{3}$	0.152×10^{2}	$-0.312\,681\,77\times10^{-2}$
0.400×10^{1}	$0.136\,327\,69\times10^{3}$	0.156×10^{2}	$-0.437\,046\,23\times10^{-2}$
0.800×10^{1}	$0.122\,654\,71\times10^{3}$	0.160×10^{2}	$-0.317\,965\,43\times10^{-2}$
0.120×10^{1}	$0.101\,731\,82\times10^{3}$	0.164×10^{2}	$-0.891\,470\,95\times10^{-3}$
0.160×10^{1}	$0.765\,663\,44\times10^{2}$	0.168×10^{2}	$0.103\,156\,22\times10^{-2}$
0.200×10^{1}	$0.511\,079\,89\times10^{2}$	0.172×10^{2}	$0.197\,404\,64\times10^{-2}$
0.240×10^{1}	$0.292\,016\,04\times10^{2}$	0.176×10^{2}	$0.200\,632\,60\times10^{-2}$
0.280×10^{1}	$0.133\,344\,57\times10^{2}$	0.180×10^{2}	$0.134\,426\,39\times10^{-2}$
0.320×10^{1}	$0.394\,328\,99\times10^{1}$	0.184×10^{2}	$0.239\,616\,71\times10^{-3}$
0.360×10^{1}	$-0.294\,886\,34$	0.188×10^{2}	$-0.854\,170\,25\times10^{-3}$
0.400×10^{1}	$-0.144\,898\,52\times10^{1}$	0.192×10^{2}	$-0.139\,990\,77\times10^{-2}$
0.440×10^{1}	$-0.129\,741\,32\times10^{1}$	0.196×10^{2}	$-0.117\,753\,33\times10^{-2}$
0.480×10^{1}	$-0.837\,909\,43$	0.200×10^{2}	$-0.459\,969\,17\times10^{-3}$
0.520×10^{1}	$-0.406\,007\,13$	0.204×10^{2}	$0.264\,586\,74\times10^{-3}$
0.560×10^{1}	$-0.533\,300\,23\times10^{-1}$	0.208×10^{2}	$0.681\,026\,02\times10^{-3}$
0.600×10^{1}	$0.188\,673\,58$	0.212×10^{2}	$0.748\,524\,90\times10^{-3}$
0.640×10^{1}	$0.273\,664\,36$	0.216×10^{2}	$0.548\,674\,90\times10^{-3}$
0.680×10^{1}	$0.208\,836\,09$	0.220×10^{2}	$0.174\,185\,50\times10^{-3}$
0.720×10^{1}	$0.738\,993\,55\times10^{-1}$	0.224×10^{2}	$-0.241\,190\,39\times10^{-3}$
0.760×10^{1}	$-0.376\,688\,32\times10^{-1}$	0.228×10^{2}	$-0.510\,576\,89\times10^{-3}$
0.800×10^{1}	$-0.820\,674\,86\times10^{-1}$	0.232×10^{2}	$-0.504\,247\,87\times10^{-3}$
0.840×10^{1}	$-0.724\,445\,68\times10^{-1}$	0.236×10^{2}	$-0.262\,329\,19\times10^{-3}$
0.880×10^{1}	$-0.418\,120\,63\times10^{-1}$	0.240×10^{2}	$0.421\,259\,24\times10^{-4}$
0.920×10^{1}	$-0.109\,476\,33\times10^{-1}$	0.244×10^{2}	$0.250\,652\,41\times10^{-3}$
0.960×10^{1}	$0.140\,131\,03\times10^{-1}$	0.248×10^{2}	$0.312\,730\,35\times10^{-3}$
0.100×10^{2}	$0.294\,143\,69\times10^{-1}$	0.252×10^{2}	$0.256\,758\,25\times10^{-3}$
0.104×10^{2}	$0.302\,637\,49\times10^{-1}$	0.256×10^{2}	$0.123\,960\,99\times10^{-3}$
0.108×10^{2}	$0.168\,266\,45\times10^{-1}$	0.260×10^{2}	$-0.447\,289\,15\times10^{-4}$
0.112×10^{2}	$-0.183\,854\,72\times10^{-2}$	0.264×10^{2}	$-0.188\,416\,47\times10^{-3}$
0.116×10^{2}	$-0.142\,996\,79\times10^{-1}$	0.268×10^{2}	$-0.239\,910\,26\times10^{-3}$
0.120×10^{2}	$-0.157\,117\,39\times10^{-1}$	0.272×10^{2}	$-0.175\,324\,89\times10^{-3}$
0.124×10^{2}	$-0.952\,986\,81\times10^{-2}$	0.276×10^{2}	$-0.384\,672\,02\times10^{-4}$
0.128×10^{2}	$-0.194\,027\,91\times10^{-2}$	0.280×10^{2}	$0.925\,379\,31\times10^{-4}$
0.132×10^{2}	$0.349\,352\,43\times10^{-2}$	0.284×10^{2}	$0.159\,975\,64\times10^{-3}$
0.136×10^{2}	$0.623\,855\,36\times10^{-2}$	0.288×10^{2}	$0.151\,294\,85\times10^{-3}$
0.140×10^{2}	$0.648\,253\,99\times10^{-2}$	0.292×10^{2}	$0.867\,844\,56\times10^{-4}$
0.144×10^{2}	$0.424\,512\,04\times10^{-2}$	0.296×10^{2}	$-0.148\,912\,39\times10^{-5}$
0.148×10^{2}	$0.364\,433\,15\times10^{-3}$	0.300×10^{2}	$-0.803\,735\,67\times10^{-4}$

where $\langle V(|\vec{R}_i-\vec{R}_j|)\rangle$ is calculated with the prescription given in Eq. (2.5) [through a Fourier-transformed $V(q)$ given in Table II], and $\omega_{\vec{k}\lambda}$ are the self-consistent phonons. This free energy is a parametric function of both T and a. For a given T, the equilibrium lattice spacing a_0 is obtained by varying a and finding the minimum of $F_{\rm SCP}$. Figure 3 (in Sec. IV) shows the behavior of $F_{\rm SCP}$ as a function of the lattice spacing. It is seen that $F_{\rm SCP}$ generally has a local physical minimum, then a local maximum, and then a "runaway" descent, which eventually terminates at some large lattice spacing where one or more phonon branches become imaginary. This latter runaway's "explosive" instability comes from the logarithmic divergence in the vibrational entropy term in Eq. (2.12) which occurs when the frequency becomes zero. This divergence is unphysical since it comes from the artificial entropy divergence $S\sim-\ln(\beta\hbar\omega)$, which occurs if $\omega\to 0$ while insisting on a harmonic treatment, which is, of course, wrong. The local minimum obtained at $a=a_0(T)$ corresponds to the stable configuration of the crystal at temperature T, and when this local minimum disappears we say that the crystal has become unstable, and the corresponding temperature at which it occurs is called the bulk instability temperature T_B. At $T=0$ the minimum of $F_{\rm SCP}$ occurs at an $a=a_0(0)$ value only very slightly larger than $\sqrt{2}R_0$, where R_0 is the position at which the pair potential has a minimum. The slight expansion $[a_0(0)-\sqrt{2}R_0]/\sqrt{2}R_0$ is due to zero-point motion and amounts to 0.4% in copper, which is negligible for all purposes.

The quasiharmonic method is similar in spirit to the SCP method and calculations are analogous to those just described, except that all thermal averages are not evaluated explicitly but are instead replaced by their value in the most probable configuration, e.g.,

$$\langle\alpha(R)\rangle\underset{\rm QH}{\to}\alpha(\langle R\rangle)\ . \tag{2.13}$$

In particular, the quasiharmonic free energy (which is no longer variational) is given by

$$F_{\rm QH}=\tfrac{1}{2}\sum_{i,j}V(\langle|\vec{R}_i-\vec{R}_j|\rangle)+\beta^{-1}\sum_{\vec{k},\lambda}\ln 2\sinh\left[\frac{\beta\hbar\omega_{\vec{k}\lambda}}{2}\right]. \tag{2.14}$$

III. CHOICE OF THE PAIR POTENTIAL

Several short-ranged potentials have been given in the literature for copper.[13–15] Unfortunately, they turn out to be unsuitable for describing thermal properties, although they have been used successfully in various other contexts. They tend to be very deep potentials which generally yield unreasonably small anharmonicities, and thus very poor expansion coefficients. Furthermore, we can easily handle a spherical potential, so any nonspherical potential found in the literature must be spherically averaged before using it for our calculation. Ercolessi[17] has verified by molecular dynamics that, for example, a spherical average of the potential of Ref. 13 leads to a bcc rather than a fcc crystal, and therefore has to be discarded at the outset.

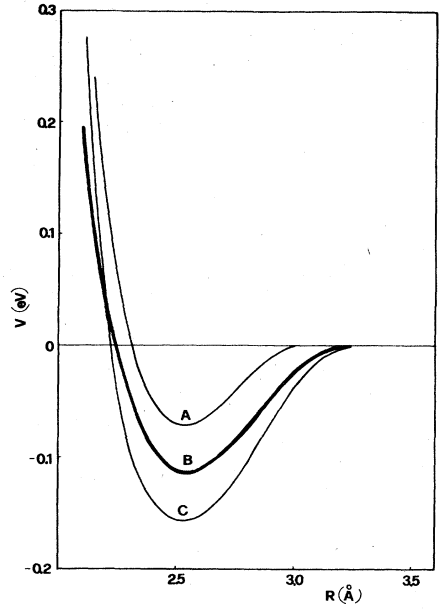

FIG. 1. Pair potential (B) for copper used in our calculation, compared with other potentials (A and C) also examined by us.

We therefore had to construct our own empirical potential for copper. It was chosen to be short ranged, with a minimum at a distance R_0 very close to the $T=0$ first-neighbor distance $a_0/\sqrt{2}$. Apart from this, it had to (i) yield a reasonable fit of the room-temperature phonons of copper; (ii) lead to a reasonable thermal expansion in the entire temperature range 0 K to T_M; and (iii) give similar results with both SCP and QH theories. The SCP thermal properties for a given potential $V(R)$ generally depend upon its *global* form, i.e., on $V(R)$ at all R around the equilibrium value $R_0(T)$, within a range which is quite large at high temperatures. On the other hand, the QH thermal properties are very sensitively dependent upon the potential behavior *at* the equilibrium distance $V(R_0(T))$. A small change of V near R_0 will thus leave the SCP results unchanged, but will be felt very strongly in the QH calculations. It is therefore reasonable and easy to adjust, by trial and error, the actual form of $V(R)$ near $R_0=a_0/\sqrt{2}$, so that SCP and QH results agree. In other words, a disagreement between QH and SCP is not a necessity and can be eliminated to yield a simple yet accurate QH calculation. Figure 1 shows three typical potential curves among the many examined. The final choice was made by trial and error, as illustrated in Fig. 2. This figure shows that the predicted thermal expansions of potential B in SCP and QH are sufficiently close to the experiment below $T=1350$ K and sufficiently similar to each other (note the expanded scale) to justify the adoption of this potential in the present work. The Fourier coefficients of this potential are given in Table II.

As mentioned in the Introduction, we note that this potential is extremely shallow, particularly if one compares its contribution to cohesion, $6|V(R_0)|\simeq 0.72$ eV, with the actual cohesive energy per atom, 3.49 eV. The vast quantity of arbitrariness implied in our procedure of con-

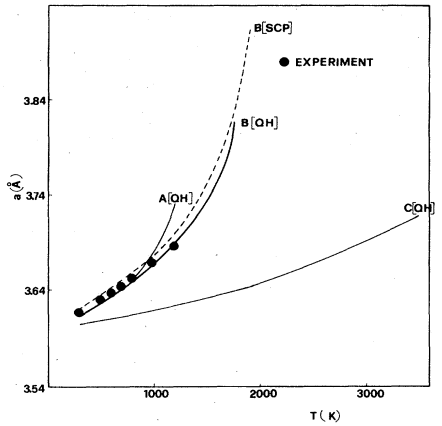

FIG. 2. Calculated lattice spacing as a function of temperature for the potentials A, B, and C. For the model potential (B), the results obtained from both QH and SCP are shown, while for others the result obtained from QH alone is shown.

struction might well allow this discrepancy to be reduced. On the other hand, as discussed in the Introduction, these two numbers are expected to disagree on physical grounds, differing only by an unknown volume cohesive term. When this calculation was completed, a molecular-dynamics test[17] showed that potential B does indeed yield a fcc crystal, with a melting temperature of about 1000 K, in fair agreement with that of copper, $T_M = 1356$ K.

IV. RESULTS AND DISCUSSIONS

Figure 3 illustrates our results for free energies of copper obtained with SCP and QH calculations. It is seen that the vibrational lattice instability occurs at about 1900 K in SCP and at 1750 K in QH, as signified by the disappearance of the minimum in the free-energy curve. We note that, while these temperatures are clearly larger than the melting temperature, 1356 K, they are still in the same order of magnitude.

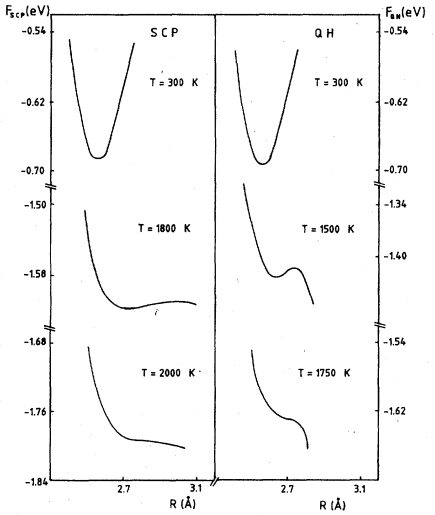

FIG. 3. Free energy (SCP and QH) as a function of the first-neighbor distance for various temperatures.

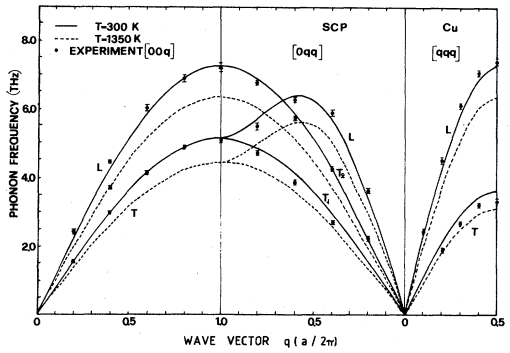

FIG. 4. Phonon spectrum of copper in SCP for $T = 300$ and 1350 K.

The shift in the position of the free-energy minimum with increasing temperatures leads to the crystal expansion of Fig. 2. We note that the calculated expansion becomes very nonlinear at high temperatures, preceding the instability. The experimental expansion, on the other hand, remains rather linear all the way up to melting. We suspect that the many-body forces, which are not included here, do in fact play a role in preventing even the small amount of nonlinear expansion predicted by our calculation below T_M from taking place.

Figure 4 shows the self-consistent phonon spectrum calculated at room temperature and just before melting. A general softening of all branches is observed, with no particular preferential effects. We have singled out, in particular, two zone-boundary modes, whose temperature-dependent frequencies are shown in Fig. 5. A similar T dependence is found for the sound velocities, as shown in Fig. 6. The general behavior of all these quantities is such that they decrease initially linearly with temperature, and

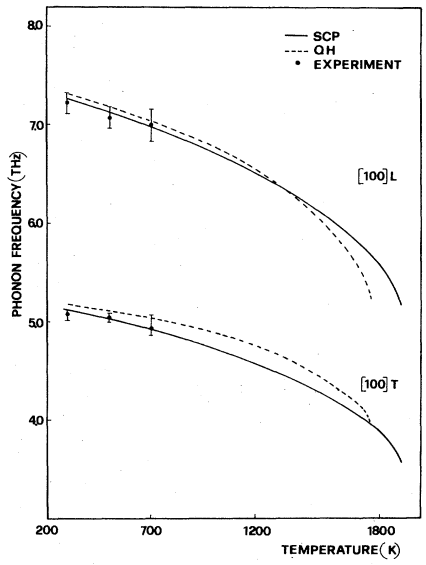

FIG. 5. Temperature dependence of zone-boundary phonon frequencies of copper, $\vec{q} = (2\pi/a)(1,0,0)$ for both SCP and QH calculations.

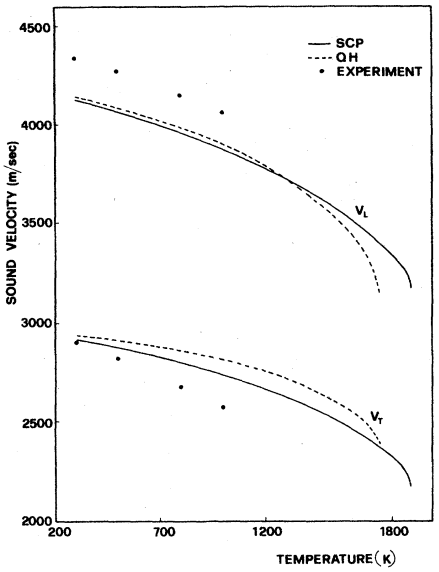

FIG. 6. Temperature-dependent [100] sound velocities calculated with SCP and QH.

then progressively faster. The total decrease at the instability is generally on the order of 20% of the $T=0$ value.

We have also calculated the mean-square vibration amplitude of an atom $\langle |u_i|^2 \rangle$ as well as the mean-square interatomic displacement $\langle |u_i - u_j|^2 \rangle$, both of which are shown in Figs. 7 and 8, respectively. Once again, $\langle u_i^2(T) \rangle$ is linear at low T and then develops a strongly increasing slope near the instability. This is reminiscent of the simplest version of self-consistent Einstein theory,[12] where the instability condition is

$$2Q^2\langle u^2 \rangle = 2Q^2 \frac{k_B T_I}{C_0} e^{2Q^2\langle u^2 \rangle} = 1 \tag{4.1}$$

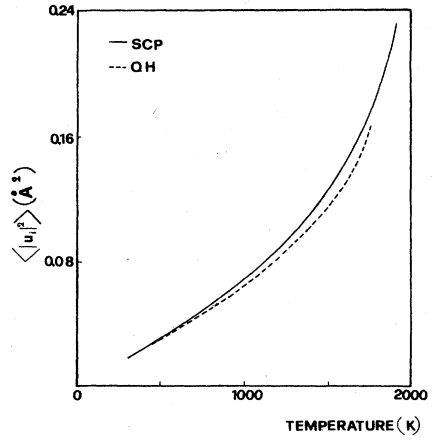

FIG. 7. Mean-square displacement of an atom (in Å^2) as a function of temperature (SCP and QH). To verify that the instability occurs roughly when predicted by Lindemann, note that $a^2(T=1750\ \text{K}) = 14.5\ \text{Å}^2$.

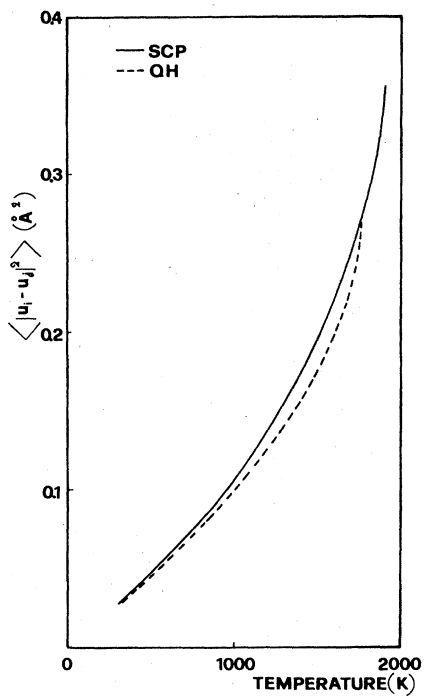

FIG. 8. Mean-square interatomic displacement as a function of temperature (SCP and QH).

(C_0 being the spring constant, and $Q \sim \pi/a$), implying an infinite slope, $\partial/\partial T \langle \omega^2 \rangle \propto \text{const} \times (T - T_I)^{-1/2}$. Another similarity suggested by Eq. (4.1) is that to the Lindemann melting criterion $(\langle u^2 \rangle)^{1/2}/a \sim 0.1 \div 0.2$, independent of mass and forces. Figure 7 indicates that a similar ratio is obtained in our calculation, with a value close to 0.11 at the instability temperature.

In conclusion, we have used the self-consistent phonon method and the quasiharmonic method to investigate the thermal properties of copper. In particular, the temperature-dependent phonon spectrum, crystal expansion, mean-square displacement, and vibrational free energy have been evaluated explicitly. A model pair potential for copper has been specially constructed for the present investigation, which was required to give similar results in SCP and QH. Having obtained this result for the bulk, one could use the simpler QH scheme for more complex studies involving surfaces and defects with confidence. The vibrational lattice instability of the crystal has also been investigated and is found to be qualitatively similar to that predicted by the simple self-consistent Einstein model.

ACKNOWLEDGMENTS

We are extremely grateful to F. Ercolessi for telling us about his unpublished molecular-dynamics results obtained with various model potentials of copper. This work was supported by the Gruppo Nazionale di Struttura della Materia del Consiglio Nazionale delle Ricerche, and also by the Ministero della Pubblica Istruzione, Italy.

APPENDIX A

We show that, to second order in displacement, the factorization of

$$\left\langle (\beta-\alpha)\frac{R_\mu R_\nu}{|R|^2}\right\rangle \rightarrow \langle \beta-\alpha\rangle \left\langle \frac{R_\mu R_\nu}{|R|^2}\right\rangle \tag{A1}$$

is correct.

We first expand in powers of u,

$$\beta-\alpha=(\beta_0-\alpha_0)+\sum_\lambda R^0(\beta_0'-\alpha_0')u_\lambda+\tfrac{1}{2}\sum_\lambda(\beta_0'-\alpha_0')u_\lambda u_\lambda+\tfrac{1}{2}\sum_{\lambda,\mu}[(\beta_0'''-\alpha_0''')-(\beta_0'-\alpha_0')]\frac{R_\lambda^0 R_\mu^0}{|R^0|^2}u_\lambda u_\mu \tag{A2}$$

and

$$\frac{R_\lambda R_\mu}{|R|^2}=\frac{R_\lambda^0 R_\mu^0+u_\lambda R_\mu^0+u_\mu R_\lambda^0+u_\mu u_\lambda}{|R^0|^2}\left[1-\frac{|u|^2}{|R^0|^2}-2\frac{(\vec{R}^0\cdot\vec{u})}{|R^0|^2}+4\frac{(\vec{R}^0\cdot\vec{u})^2}{|R^0|^4}\right], \tag{A3}$$

where

$$\alpha_0'=\frac{1}{|R|}\frac{\partial\alpha}{\partial|R|}\ ,\quad \beta_0'=\frac{1}{|R|}\frac{\partial\beta}{\partial|R|}\ ,\quad \alpha_0''=\frac{\partial^2\alpha}{\partial|R|^2}\ ,\quad \text{and } \beta_0''=\frac{\partial^2\beta}{\partial|R|^2}$$

are all evaluated at equilibrium position. Using Eqs. (A2) and (A3) it can be seen that, to second order in u, the difference between the left- the right-hand sides of Eq. (A1) results from the cross product

$$\left\langle\left[\sum_\nu R_\nu^0 u_\nu(\beta_0'-\alpha_0')\right]\left[\frac{u_\lambda R_\mu^0}{|R^0|^2}+\frac{u_\mu R_\lambda^0}{|R^0|^2}-\frac{2(\vec{R}^0\cdot\vec{u})}{|R^0|^2}\frac{R_\lambda^0 R_\mu^0}{|R^0|^2}\right]\right\rangle\equiv X\ . \tag{A4}$$

Consider case (i), where $\lambda=\mu=x$; then

$$\begin{aligned}X=&\frac{2(\beta_0'-\alpha_0')}{|R^0|^2}(R_x^{02}\langle u_x^2\rangle+R_x^0R_y^0\langle u_xu_y\rangle+R_x^0R_z^0\langle u_xu_z\rangle)\\&-\frac{2(\beta_0'-\alpha_0')}{|R^0|^2}\left[\frac{R_x^{02}}{|R^0|^2}(R_x^{02}\langle u_x^2\rangle+R_y^{02}\langle u_y^2\rangle+R_z^{02}\langle u_z^2\rangle)\right.\\&\left.+\frac{2R_x^{02}}{|R^0|^2}(R_x^0R_y^0\langle u_xu_y\rangle+R_x^0R_z^0\langle u_xu_z\rangle+R_y^0R_z^0\langle us_yu_z\rangle)\right].\end{aligned} \tag{A5}$$

We note that for a fcc crystal with first-neighbor interaction, the cross term X is zero since

$$R_x^{02}\langle u_x^2\rangle=\frac{R_x^{02}}{|R^0|^2}(R_x^{02}\langle u_x^2\rangle+R_y^{02}\langle u_y^2\rangle+R_z^2\langle u_z^2\rangle)$$

and

$$R_x^0R_y^0\langle u_xu_y\rangle+R_x^0R_z^0\langle u_xu_z\rangle=\frac{2R_x^{02}}{|R^0|^2}(R_x^0R_y^0\langle u_xu_y\rangle+R_x^0R_z^0\langle u_xu_z\rangle+R_y^0R_z^0\langle u_yu_z\rangle)\ . \tag{A6}$$

TABLE III. Thermal average of various types of displacement correlations calculated using Eq. (2.9). Calculations are done at $T=500$ K, and units are Å^2.

$\vec{R}^0$	$\langle u_x,u_x\rangle$	$\langle u_x,u_y\rangle$	$\langle u_x,u_z\rangle$	$\langle u_y,u_z\rangle$	$\langle\|u\|^2\rangle$
(−1,1,0)	0.015 98	0.002 09	0	0	0.046 59
(−1,−1,0)	0.015 98	−0.002 09	0	0	0.046 59
(1,−1,0)	0.015 98	0.002 09	0	0	0.046 59
(1,1,0)	0.015 98	−0.002 09	0	0	0.046 59
(1,0,1)	0.015 98	0	−0.002 09	0	0.046 59
(1,0,−1)	0.015 98	0	0.002 09	0	0.046 59
(−1,0,−1)	0.015 98	0	−0.002 09	0	0.046 59
(−1,0,1)	0.015 98	0	0.002 09	0	0.046 59
(0,1,1)	0.016 40	0	0	−0.002 09	0.046 59
(0,−1,1)	0.016 40	0	0	0.002 09	0.046 59
(0,−1,−1)	0.016 40	0	0	−0.002 09	0.046 59
(0,1,−1)	0.016 40	0	0	0.002 09	0.046 59

This result is due to symmetry and is evident if one looks at the first-neighbor positions of a fcc crystal, and at the corresponding thermal average of various displacements that are given in Table III. By symmetry, $X=0$ also for $\lambda=\mu=y$ or z.

Consider now case (ii), where $\lambda\neq\mu$, and, for instance, $\lambda=x$ and $\mu=y$; then

$$X=\frac{\beta_0'-\alpha_0'}{|R^0|^2}[R_x^0R_y^0(\langle u_x^2\rangle+\langle u_y^2\rangle)+(R_x^{02}+R_y^{02})\langle u_xu_y\rangle+R_x^0R_z^0\langle u_yu_z\rangle+R_y^0R_z^0\langle u_xu_z\rangle]$$
$$-\frac{2(\beta_0'-\alpha_0')}{|R^0|^2}\left[\frac{R_x^0R_y^0}{|R^0|^2}(R_x^{02}\langle u_x^2\rangle+R_y^{02}\langle u_y^2\rangle+R_z^{02}\langle u_z^2\rangle+2R_x^0R_y^0\langle u_xu_y\rangle+2R_x^0R_z^0\langle x_xu_z\rangle+2R_y^0R_z^0\langle u_yu_z\rangle)\right]. \quad \text{(A7)}$$

We note, as before, that X is zero, because

$$R_x^0R_y^0(\langle u_x^2\rangle+\langle u_y^2\rangle)=\frac{2R_x^0R_y^0}{|R^0|^2}(R_x^0\langle u_x^2\rangle+R_y^{02}\langle u_y^2\rangle+R_z^{02}\langle u_z^2\rangle),$$
$$(R_x^{02}+R_y^{02})\langle u_xu_y\rangle=\frac{4R_x^{02}R_y^{02}}{|R^0|^2}\langle u_xu_y\rangle, \quad \text{(A8)}$$
$$R_x^0R_z^0\langle u_yu_z\rangle=R_y^0R_z^0\langle u_xu_z\rangle=0,$$

and

$$R_x^{02}R_yR_z\langle u_xu_z\rangle=R_x^{02}R_y^{02}R_z\langle u_yu_z\rangle=0, \quad \text{(A9)}$$

as can be seen from Table III and by looking at the first-neighbor positions. From this we can conclude that the cross product X is, in general, zero, and the factorization given in Eq. (A1) is true up to second order in displacement.

APPENDIX B

Here we explicitly give the dynamical matrix for a fcc crystal used in the self-consistent phonon calculation:

$$\begin{aligned}
D_{xx}&=4(\langle\beta\rangle+2\langle\alpha\rangle)+4\langle\beta-\alpha\rangle(B+2C-2D)-4\cos(\pi q_y)\cos(\pi q_z)(\langle\alpha\rangle+B\langle\beta-\alpha\rangle)\\
&\quad-2\cos(\pi q_x)[\cos(\pi q_y)+\cos(\pi q_z)](\langle\beta+\alpha\rangle+2C\langle\beta-\alpha\rangle-2D\langle\beta-\alpha\rangle),\\
D_{yy}&=4(\langle\beta\rangle+2\langle\alpha\rangle)+4\langle\beta-\alpha\rangle(B+2C-2D)-4\cos(\pi q_x)\cos(\pi q_z)(\langle\alpha\rangle+B\langle\beta-\alpha\rangle)\\
&\quad-2\cos(\pi q_y)[\cos(\pi q_x)+\cos(\pi q_z)](\langle\beta+\alpha\rangle+2C\langle\beta-\alpha\rangle-2D\langle\beta-\alpha\rangle),\\
D_{zz}&=4(\langle\beta\rangle+2\langle\alpha\rangle)+4\langle\beta-\alpha\rangle(B+2C-2D)-4\cos(\pi q_x)\cos(\pi q_y)(\langle\alpha\rangle+B\langle\beta-\alpha\rangle)\\
&\quad-2\cos(\pi q_z)[\cos(\pi q_x)+\cos(\pi q_y)](\langle\beta+\alpha\rangle+2C\langle\beta-\alpha\rangle-2D\langle\beta-\alpha\rangle),\\
D_{xy}&=2\langle\beta-\alpha\rangle\sin(\pi q_x)\sin(\pi q_y)(1-2A-2D),\\
D_{xz}&=2\langle\beta-\alpha\rangle\sin(\pi q_x)\sin(\pi q_z)(1-2A-2D),\\
D_{yz}&=2\langle\beta-\alpha\rangle\sin(\pi q_y)\sin(\pi q_z)(1-2A-2D),
\end{aligned} \quad \text{(B1)}$$

where

$$A=\frac{|\langle u_xu_x\rangle|}{a_0^2/2}$$

is calculated for the neighbor $(a_0/2)(1,1,0)$,

$$B=\frac{|\langle u_xu_x\rangle|}{a_0^2/2}$$

is calculated for the neighbor $(a_0/2)(0,1,1)$,

$$C=\frac{|\langle u_xu_y\rangle|}{a_0^2/2}$$

is calculated for the neighbor $(a_0/2)(1,1,0)$, and

$$D=\frac{\langle|u|^2\rangle}{a_0^2}.$$

The first step of the calculation is done by taking $\langle\alpha\rangle=\alpha=0$, $\langle\beta\rangle=\beta$, and $B,C,D=0$.

*Present address: Centre d'Etudes Nucléaires Saclay, DphG Service de Physique des Atomes et Surfaces, 91191 Gif-sur-yvette, France.

[1]See, e.g., N. R. Werthamer, in *Rare Gas Solids,* edited by M. L. Klein and J. A. Venables (Academic, New York, 1976), p. 266.

[2]J. A. Moriarty, Phys. Rev. B **6**, 1239 (1972).

[3]L. Dagens, J. Phys. F **7**, 1167 (1977).

[4]O. P. Sharma, Phys. Status Solidi B **86**, 483 (1978).

[5]R. H. Rautioaho, Phys. Status Solidi B **112**, 391 (1982).

[6]S. S. Jaswal and L. A. Girifalco, J. Phys. Chem. Solids **28**, 457 (1967).

[7]E. R. Cowley and R. C. Shukla, Phys. Rev. B **9**, 1261 (1974).

[8]C. S. Jayanthi, E. Tosatti, A. Fasolino, and L. Pietronero, in Proceedings of the VIth ECOSS Conference, York, 1984 [Surf. Sci. (to be published)]; C. S. Jayanthi, E. Tosatti, and L. Pietronero (unpublished).

[9]P. Choquard, *The Anharmonic Crystal* (Benjamin, New York, 1967).

[10]L. K. Moleko and H. R. Glyde, Phys. Rev. B **27**, 6019 (1983).

[11]See, e.g., L. L. Boyer, Phys. Rev. Lett. **42**, 584 (1979); Y. Ida, Phys. Rev. **187**, 951 (1969).

[12]L. Pietronero and E. Tosatti, Solid State Commun. **32**, 255 (1979).

[13]R. A. Johnson and W. D. Wilson, in *Interatomic Potentials and Simulation of Lattice Defects,* edited by P. C. Gehlen, J. R. Beeler, and R. J. Jaffee (Plenum, New York, 1972), p. 301.

[14]M. J. Baskes and C. F. Melius, Phys. Rev. B **8**, 3197 (1979).

[15]S. W. de Leeuw, M. Dixon, and R. J. Elliott, Philos. Mag. A **46**, 677 (1982).

[16]A. Baldereschi, Phys. Rev. B **7**, 5212 (1973); D. J. Chadi and M. L. Cohen, *ibid.* **8**, 5747 (1973).

[17]F. Ercolessi (private communication).